

## The role of nonlinearities associated with air-sea coupling processes in El Nino's peak-phase locking

DUAN WanSuo<sup>1\*</sup>, ZHANG Rui<sup>1,2</sup>, YU YanShan<sup>3</sup> & TIAN Ben<sup>1,2</sup>

<sup>1</sup>LASG, Institute of Atmospheric Physics, Chinese Academy of Sciences, Beijing 100029, China;

<sup>2</sup>Graduate University of Chinese Academy of Sciences, Beijing 100049, China;

<sup>3</sup>Institute of Ocean, Chinese Academy of Sciences, Qingdao 266071, China

Received June 21, 2012; accepted February 10, 2013

We use conditional nonlinear optimal perturbation (CNOP) to investigate the optimal precursory disturbances in the Zebiak-Cane El Nino-Southern Oscillation (ENSO) model. The conditions of the CNOP-type precursors are highly likely to evolve into El Nino events in the Zebiak-Cane model. By exploring the dynamic behaviors of these nonlinear El Nino events caused by the CNOP-type precursors, we find that they, as expected, tend to phase-lock to the annual cycles in the Zebiak-Cane model, with the SSTA peak at the end of a calendar year. However, El Nino events with CNOPs as initial anomalies in the linearized Zebiak-Cane model are inclined to phase-lock earlier than nonlinear El Nino events despite the existence of annual cycles in the model. It is clear that nonlinearities play an important role in El Nino's phase-locking. In particular, nonlinear temperature advection increases anomalous zonal SST differences and anomalous westerlies, which weakens anomalous upwelling and acts on the increasing anomalous vertical temperature difference and, as a result, enhances El Nino and then delays the peak SSTA. Finally, we demonstrate that nonlinear temperature advection, together with the effect of the annual cycle, causes El Nino events to peak at the end of the calendar year.

**El Nino event, nonlinearity, optimal perturbation, numerical model**

**Citation:** Duan W S, Zhang R, Yu Y S, et al. The role of nonlinearities associated with air-sea coupling processes in El Nino's peak-phase locking. *Science China: Earth Sciences*, 2013, doi: 10.1007/s11430-013-4629-y

The El Nino/Southern Oscillation (ENSO) phenomenon, originated in the Tropical Pacific, is the strongest natural interannual climate signal and has widespread effects on the global climate system and the ecology of the Tropical Pacific. Any strong change in ENSO statistics will have serious climatic and ecological consequences. It is therefore very important to simulate and predict ENSO (Latif et al., 1998; Kirtman et al., 2002; Chen et al., 2004). Critical to this process is a good understanding of ENSO (Neelin, 1991; Wang and Fang, 1996; Jin, 1997a, b; Wang, 2001).

ENSO's spatial features, temporal evolutions, and rela-

tionships with oceanic and atmospheric variables have been clearly defined (Wallace et al., 1998). ENSO has irregular periods of 2–7 years, with the average being approximately 3–4 years (Quinn et al., 1987), typically lasts 12–18 months, and is accompanied by changes in the Southern Oscillation (Bjerknes, 1969), an interannual mass exchange between the Eastern (Asian-Australia monsoon region) and Western (Pacific trade wind region) Hemispheres (Walker, 1924). Mature phases of warm episodes tend to occur in boreal winter (Mitchell and Wallace, 1996). Furthermore, most ENSO warm events occur with thermocline deepening in the east and thermocline shallowing in the west along the equator, and a phase leading of the thermocline transition to SST prior to the peak of the ENSO event (Wang and Fang,

\*Corresponding author (email: duanws@lasg.iap.ac.cn)

1996; Duan et al., 2004). Usually, the persistence of the Southern Oscillation declines during boreal spring, and the weakest persistence of ENSO thus occurs in boreal spring (Webster and Yang, 1992; Clark and Van Gorder, 1999; Mu et al., 2007a, b). In addition, the transition of ENSO from a cold event to a warm event often occurs in boreal spring, or vice versa (Mitchell and Wallace, 1996). In particular, the ENSO tends to result in the peak activity of El Nino and La Nina occurring at the end of the calendar year (Tziperman et al., 1994; Chang et al., 1994, 1995; Wang and Fang, 1996; Wang et al., 1999).

Phase-locking is one of the predominant characteristics of ENSO (Rasmusson and Carpenter, 1982). The mechanism leading to the preferred boreal winter occurrence of the ENSO warm phase has been previously discussed (Battisti and Hirst, 1989). Tziperman et al. (1997) showed that the phase-locking of El Nino's peak is dominated by basic-state wind divergence associated with the seasonal movement of the tropical convergence zone. Tziperman et al. (1998) further noted that seasonally varying amplification of Rossby and Kelvin waves caused by coupled instability can force an El Nino event to mature when this amplification is at its minimum strength during boreal winter. Neelin et al. (2000) investigated ENSO phase-locking variations and demonstrated that scattered phase-locking behavior is seen in both observations and models. The authors showed that the mechanism underlying the scattered phase-locking behavior resulted from competition between the inherent ENSO frequency and the tendency to phase-lock to the preferred season because of a nonlinear interaction between the annual and ENSO cycles. In particular, An and Wang (2001) used a modified Zebiak-Cane model (Zebiak and Cane, 1987) to show that the ENSO's phase-locking to the annual cycle was due to seasonally varying basic states. Importantly, these studies focus primarily on the effect of the climatological annual cycle on ENSO phase-locking. In fact, nonlinearities associated with air-sea coupling processes also have significant contributions to the ENSO's phase-locking (see section 3 in current study). Then we naturally ask the following questions: what is the role of the nonlinearities in ENSO's phase-locking? How do the nonlinearities modulate ENSO phase-locking? Furthermore, several nonlinear processes exist in coupled ENSO systems. For example, in the Zebiak-Cane model, there are nonlinearities that arise from temperature advection, subsurface temperature parameterization, and wind stress anomalies. It is therefore necessary to address which nonlinear process is the dominating factor that affects ENSO phase-locking.

Here we will use conditional nonlinear optimal perturbation (CNOP) to address the role of nonlinearities in ENSO phase-locking by investigating the optimal precursory disturbance of ENSO. CNOP is the initial perturbation that satisfies a certain physical constraint and has the largest nonlinear evolution at prediction time. In ENSO predictability studies, the CNOP superimposed on the climatologi-

cal background state can describe the optimal precursory disturbance because of its maximum nonlinear evolution at the prediction time (Mu et al., 2003; Duan et al., 2004; Duan and Mu, 2006; Duan et al., 2008). In other words, the CNOP has the highest likelihood of evolving into an ENSO event and acts as the optimal precursory disturbance for this ENSO event. By investigating the behavior of the CNOP and comparing its linear counterpart, the effect of nonlinearities can be revealed. Relatedly, the CNOP approach has been applied to study the nonlinear asymmetry of El Nino and La Nina amplitudes (Duan and Mu, 2006; Duan et al., 2008). In this paper, we will apply the CNOP approach in the Zebiak-Cane model to explore the phase-locking of ENSO events caused by CNOP-type precursors in an attempt to reveal the effect of nonlinearity on the phase-locking of ENSO events. Importantly, because the Zebiak-Cane model is limited in its ability to simulate the main characteristics of La Nina (An and Wang, 2001), this paper does not address the behavior of the phase-locking of La Nina but only study that of El Nino.

## 1 The CNOP approach

The CNOP is an initial perturbation that satisfies a given physical constraint and has the largest nonlinear evolution at the prediction time (described below). The CNOP approach is a natural generalization of the linear singular vector (LSV) approach to nonlinear regime and differs from the LSV in patterns and growth (Duan and Mu, 2009). For convenience, we briefly review the CNOP approach:

Let  $M_{t_0,t}$  be the propagator (i.e., the numerical model) of a nonlinear model from initial time  $t_0$  to  $t$ .  $u_0$  is an initial perturbation superimposed on the basic state  $U(t)$ , which is a solution to the nonlinear model and satisfies  $U(t) = M_{t_0,t}(U_0)$ , where  $U_0$  is the initial value of the basic state  $U(t)$ .

For a chosen norm  $\|\cdot\|$ , the previously mentioned CNOP can be obtained by the following optimization equation.

$$J(u_{0\delta}) = \max_{\|u_0\| \leq \delta} \|M_{t_0,t}(U_0 + u_0) - M_{t_0,t}(U_0)\|, \quad (1)$$

where  $\|u_0\| \leq \delta$  is the initial constraint defined by the chosen norm  $\|\cdot\|$  and  $u_{0\delta}$  is the CNOP. The norm  $\|\cdot\|$  also measures the evolution of the perturbations. We can also investigate situations in which the initial perturbations belong to different functional sets. Furthermore, the constraint condition could reflect certain physical laws that the initial perturbation should satisfy.

The CNOP possesses clear physical meanings (Duan and Mu, 2009). As mentioned in the introduction, an obtained CNOP that is superimposed on the climatological basic state

acts as the initial anomaly mode that is most likely to evolve into an El Niño event and represents the optimal precursor of El Niño. CNOP can also be used to study the initial error that has the largest negative effect on the prediction result at the prediction time (Duan and Mu, 2009). In sensitivity analysis studies, CNOP may represent the most unstable mode and can be used to study target observations (Mu et al., 2009).

To compute CNOP, one needs to solve eq. (1). We note that eq. (1) is a maximization optimization problem and there is no method to calculate it. However, many existing methods can deal with minimization optimization problems. Therefore, eq. (1) must be transformed into a minimization problem by considering the negative of the cost function. Then, methods such as Spectral Projected Gradient 2 (SPG2; Birgin et al., 2000), Sequential Quadratic Programming (SQP; Powell et al., 1982), and Limited memory Broyden-Fletcher-Goldfarb-Shanno (L-BFGS; Liu and Nocedal, 1989) can be used to compute CNOP. In these techniques, the gradient of the modified cost function is necessary; furthermore, the adjoint of the corresponding model is typically used to obtain the gradient. With this gradient information, using these methods with initial estimations can determine the minimum of the modified cost function (i.e., the maxima of the cost function in eq. (1)) along the descendent direction of the gradient. In phase space, the point corresponding to the minimum of the modified cost function is the CNOP defined by the eq. (1). In this paper, we use the SPG2 method to obtain the CNOPs of the Zebiak-Cane model.

## 2 The Zebiak-Cane model

The Zebiak-Cane model was the first coupled ocean-atmosphere model to simulate the interannual variability of observed ENSOs and has been a benchmark in the ENSO community for over three decades. The El Niño events reproduced by the Zebiak-Cane model are very similar to the observed El Niño events (Zebiak and Cane, 1987; also see Figure 1). Furthermore, the Zebiak-Cane model has been widely used in predictability studies and for predicting ENSOs (Zebiak and Cane, 1987; Blumenthal, 1991; Xue et al., 1994; Chen et al., 2004; Tang et al., 2008).

The model consists of a Gill-type steady-state linear atmospheric model and a reduced-gravity oceanic model, and predicts anomalous quantities by prescribing basic states of the atmosphere and ocean, including the surface winds and divergence, ocean surface layer currents, the upwelling at the base of the surface layer, sea surface temperature (SST), vertical SST gradients at the bottom of the surface layer, and thermocline depth (see Zebiak and Cane, 1987).

Atmospheric dynamics in the Zebiak-Cane model are described by the steady-state linear shallow water equations on an equatorial beta plane. The circulation is driven by a heating anomaly that depends partly on local heating that is associated with SST anomalies and partly on low-level moisture convergence (parameterized in terms of the surface wind convergence; Zebiak, 1986). Here, the convergence feedback is a nonlinear process because moisture-related heating is operative only when the total wind field is

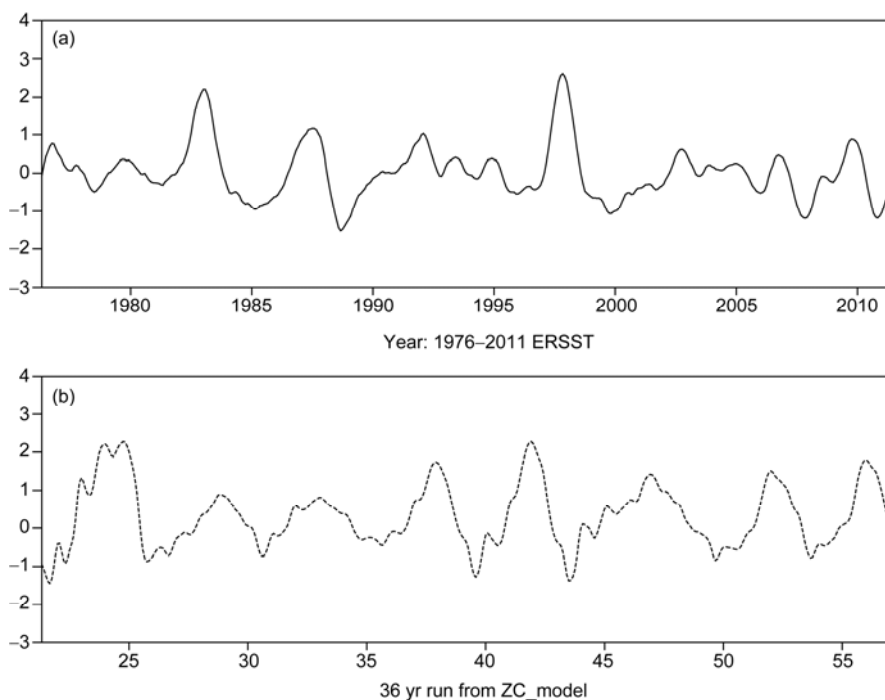


**Figure 1** (a) The observed El Niño events (derived from ERSST data) and (b) the El Niño events in the Zebiak-Cane model. It is obvious that the model El Niño events are very similar to the observed El Niño events and can be acceptable for investigating the phase-locking feature of the El Niño events.

convergent, which depends not only on the calculated convergence anomaly but also on the specified mean convergence. The important effect of this feedback is that it focuses the atmospheric response to SST anomalies into or near the regions of mean convergence, in particular, the Inter-tropical Convergence Zone and the Southern Pacific Convergence Zone.

The thermodynamics are governed by an evolution equation of the SST anomaly in the tropical Pacific that includes three-dimensional temperature advection by both the specified mean currents and the calculated anomalous currents. The assumed surface heat flux anomaly is proportional to the local SST anomaly and always acts to adjust the temperature field toward its climatological mean state, which is determined based on observations.

In the model run, the atmosphere is previously run with the specified monthly mean SST anomalies to simulate monthly mean wind anomalies. Afterwards, the ocean component is driven by surface wind stress anomalies that are generated from a combination of the surface wind anomalies produced by the atmosphere model and the background mean winds.

### 3 Results

In this section, we will use the physics of CNOP as the optimal precursory disturbance for El Nino events to investigate the behaviors of phase-locking of El Nino events, and reveal the effect of nonlinearities on phase-locking time.

#### 3.1 The optimal precursory disturbance for El Nino events

To use the Zebiak-Cane model to find the optimal precursory disturbance for an El Nino event, we construct a cost function to measure the evolution of the SSTA. The aforementioned CNOP, denoted by  $u_{0\delta}$ , can be obtained by solving eq. (2).

$$J(u_{0\delta}) = \max_{\|u_0\|_1 \leq \delta} \|T(\tau)\|_2, \quad (2)$$

where  $u_0 = (w_1^{-1}T_0, w_2^{-1}h_0)$  is a non-dimensional SSTA and a thermocline depth anomaly is superimposed on the climatological annual cycle.  $w_1=2^\circ\text{C}$  and  $w_2=50\text{ m}$  are the characteristic scales of the SST and thermocline depth.  $\|u_0\|_1 \leq \delta$  is the constraint condition defined by a prescribed positive real number  $\delta$  and the norm  $\|u_0\|_1 = \sqrt{\sum_{i,j} \{(w_1^{-1}T_{0i,j})^2 + (w_2^{-1}h_{0i,j})^2\}}$ , where  $T_{0i,j}$  and  $h_{0i,j}$  represent the dimensional SSTA and thermocline depth anomaly at different grid points and  $(i, j)$  is the grid point in the domain of the tropical Pacific with a latitude and longitude, respectively, of  $129.375^\circ\text{E}$  to  $84.375^\circ\text{W}$  by  $5.625^\circ$  and

from  $19^\circ\text{S}$  and  $19^\circ\text{N}$  by  $2^\circ$ . The evolution of the SSTA is measured by  $\|T(\tau)\|_2 = \sqrt{\sum_{i,j} (T_{i,j}(\tau))^2}$ .  $T(\tau)$  represents the evolution of SSTA at time  $\tau$  and is obtained by integrating the Zebiak-Cane model from 0 to  $\tau$  with initial anomaly  $(T_0, h_0)$ .

The CNOPs that are superimposed on the climatological annual cycles in the Zebiak-Cane model are computed for the optimization time  $\tau = 12$  months, with initial times occurring in January, April, July, and October. The constraint bounds  $\delta$  (see eq. (2)) are experimentally chosen to be 0.8, 1.0, and 1.2. For each constraint bound, similar results are obtained. Therefore, for simplicity, we use the results of  $\delta = 0.1$  to illustrate the optimal precursory disturbance for El Nino events, where  $\delta = 0.1$  means the constraint  $\|u_0\|_1 = \sqrt{\sum_{i,j} \{(w_1^{-1}T_{0i,j})^2 + (w_2^{-1}h_{0i,j})^2\}} \leq 1.0$  and implies that the initial SSTA and thermocline depth anomaly measured by the chosen norm do not exceed 1.0 (dimensional SSTA =  $2.0^\circ\text{C}$  and thermocline depth anomaly = 50 m).

Computations demonstrate that for each initial time, one CNOP of the climatological annual cycle exists. In Figure 2, we plot the CNOPs with initial times occurring in January, April, July, and October. The figure shows that these CNOPs consist of two components of the SSTA and thermocline depth anomaly; the SSTA components logically have a zonal dipolar pattern with positive anomalies in the equatorial eastern Pacific and negative anomalies in the equatorial central-western Pacific, and the thermocline depth anomaly components tend to be positive anomalies along the equator. The CNOPs' patterns imply warm subsurface water and an anomalous equatorial eastern-western thermal contrast with positive anomalies in the eastern Pacific and negative anomalies in the central-western Pacific. Such CNOP conditions tend to reduce the total zonal SST thermal contrast and increase the temperature of subsurface water, which increases westerly anomalies, suppresses anomalous upwelling, and makes the thermocline much flattening, finally inducing the onset of an El Nino event. By investigating the evolution of the CNOPs, we find that the CNOPs indeed evolve into El Nino events (also see Duan et al., 2012), which, furthermore, tend to lock their mature phase to the end of the calendar year and are consistent with observed El Nino events. Figure 3 illustrates the Nino-3 SSTA component of the evolution of the CNOPs with the initial times set to January, April, July, and October. It is shown that the El Nino events in the Zebiak-Cane model often experience a growth phase, a mature phase, and a decay phase; furthermore, the mature phase usually locks to the end of the calendar year. It is clear that the model El Nino events induced by the optimal precursory disturbances are very similar to the observed El Nino events. It is obvious that the Zebiak-Cane model is clearly acceptable for investigating the peak-phase locking of El Nino events.

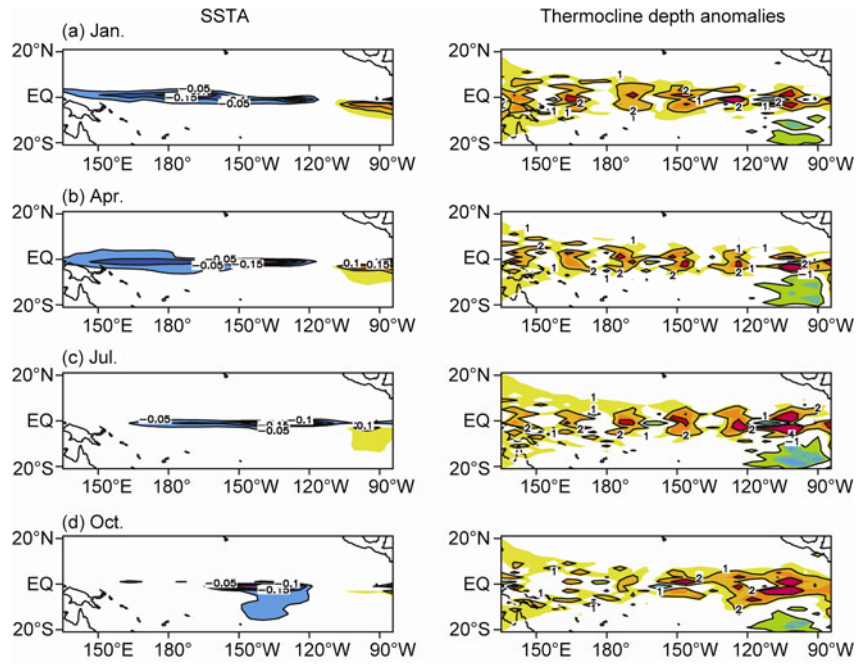


**Figure 2** The CNOPs of the climatological annual cycle with initial times occurring in January (a), April (b), July (c), and October (d). The left column shows the SSTA component, and the right column shows the thermocline depth anomalies.

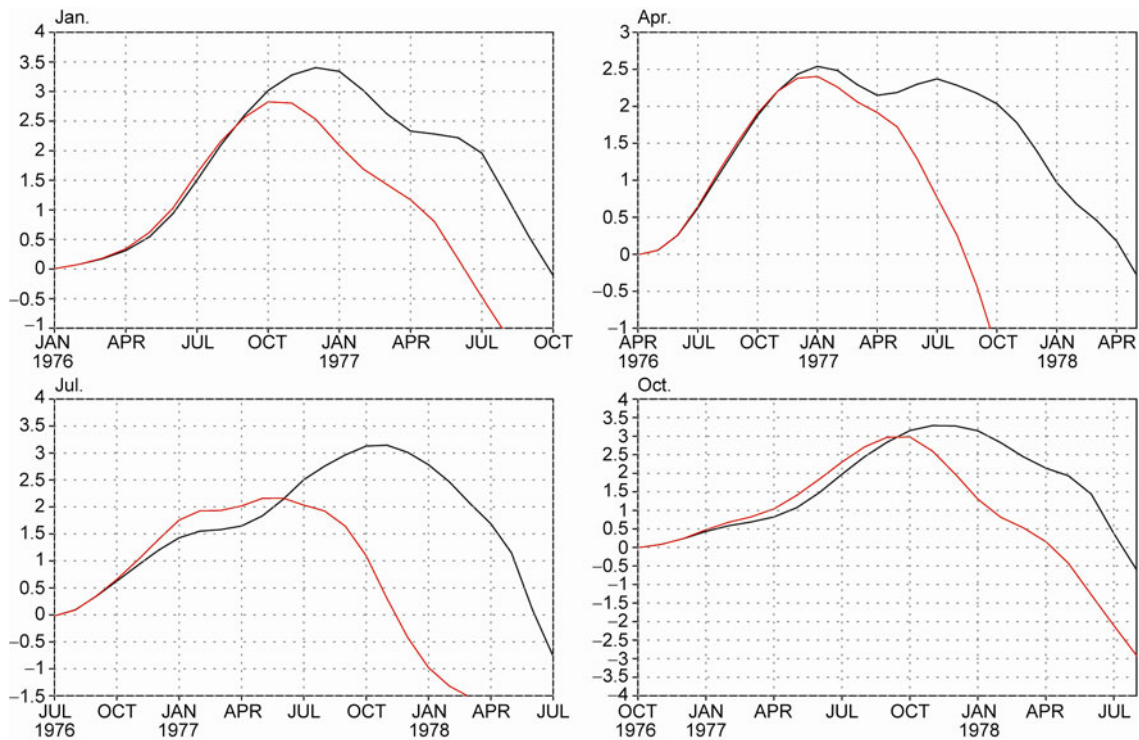


**Figure 3** The evolution of the Niño-3 SSTA component of nonlinear El Niño events with initial optimal precursors in January, April, July, and October and their linearized counterparts. The SSTAs of nonlinear El Niño events are often larger than those of the linearized El Niño events. The mature phase of the linearized El Niño events often phase-locks earlier than the nonlinear El Niño events reach their peak SSTAs. The nonlinearities postpone the maturation of the linearized El Niño events.

### 3.2 Effect of nonlinearities on El Niño phase-locking

To investigate the effect of nonlinearities on the peak-phase locking of El Niño events, we linearized the Zebiak-Cane

model and integrated it with the CNOPs as initial anomalies. Subsequently, we obtained the El Niño events in the linearized Zebiak-Cane model. For convenience, we denote these El Niño events as linearized El Niño events and refer to the

El Nino events in the Zebiak-Cane model as nonlinear El Nino events. We demonstrate that the linearized El Nino events also experience a growth phase, a mature phase, and a decay phase; however, they do not lock their mature phase to the end of the calendar year, and instead lock to a much earlier season besides the linearized El Nino events with initial time being April. For example, the linearized El Nino events with the CNOP initialized in January and October reach their SSTA peaks in October (Figure 3); and those with CNOP initialized in July attains their peak in May. These phase-locking times are earlier than peaks of the nonlinear El Nino events.

Tziperman et al. (1998), An and Wang (2001), and others have demonstrated that the phase-locking of El Nino events in the Zebiak-Cane model is due to the seasonally varying basic state. In fact, the strongest air-sea coupled instability in spring favors the growth of El Nino and the weakest coupled instability in autumn favors the decay of El Nino events, which then causes the El Nino events to reach their mature phases at the end of the year. In the linearized Zebiak-Cane model, the climatological annual cycle with the strongest (weakest) air-sea coupled instability in spring (autumn) remains in the model, whereas the resultant linearized El Nino events lock the mature phase to autumn, when the ENSO coupled system has the weakest climatological air-sea coupled instability. Therefore, the seasonally varying climatological basic state cannot completely explain why the maturation of El Nino events is typically locked to the end of the year.

It is conceivable that the differences between nonlinear El Nino events and their linearized counterparts reflect the effect of nonlinearities. It is therefore inferred that the differences between the phase-locking time of the nonlinear El Nino events and their linearized counterparts are due to the effect of nonlinearities. We have demonstrated that the linearized El Nino events phase-lock earlier than the nonlinear El Nino events attain their SSTA peaks, which implies that the nonlinearities in the Zebiak-Cane model tend to postpone the phase-locking season of El Nino events. Clearly, the nonlinearities also play an important role in the phase-locking of El Nino events beyond the climatological annual cycle.

### 3.3 Interpretations

By studying the nonlinear and linearized El Nino events, we also show that the nonlinear El Nino events are often stronger than the linearized El Nino events, which indicates that the nonlinearities increase the SSTAs and enhance the linearized El Nino events. Figure 3 shows the results associated with the enhancement of the nonlinearities on the linearized El Nino events with initial optimal precursors in January. Unsurprisingly, when the linearized El Nino events decay during the autumn (because of the weakest coupled instability), the nonlinearities increase the SSTAs and slow

their decay, finally postponing the phase-locking season of the El Nino events.

In the Zebiak-Cane model, the nonlinear effects arise from nonlinearities in temperature advections (NTA), sub-surface temperature parameterization (STP), and wind stress anomaly (WSA). For these kinds of nonlinearities, it is necessary to address how each kind of nonlinearity modulates El Nino events and which nonlinearities play a dominant role in the phase-locking of El Nino events.

To address these questions, we perform a group of sensitivity experiments. The nonlinear terms associated with NTA, WSA, and STP in the Zebiak-Cane model are respectively linearized while the other nonlinear terms remain unchanged. Then, we obtain three partially linearized Zebiak-Cane models with linearized NTA, linearized WSA, and linearized STP. For convenience, the three partially linearized models are denoted as the L-NTA model, L-WSA model, and L-STP model. Integrating these models with the CNOP as the initial condition, we obtain the corresponding evolution-patterns of the SSTAs (Figure 4). We find that the positive SSTAs of the nonlinear El Nino events are often larger than the SSTAs from the L-NTA model, but smaller than the SSTAs from the L-WSA and L-STP models. Furthermore, we demonstrate that the El Nino events in the L-WSA and L-STP models phase-lock during approximately the same season as the nonlinear El Nino events, whereas those in the L-NTA model tend to phase-lock in autumn, much like the linearized El Nino events. This result indicates that the nonlinearities in temperature advection significantly postpone the phase-locking season of the linearized El Nino events, whereas those in the sub-surface temperature parameterization and wind stress anomalies trivially affect the El Nino events' peak times. In fact, the linearization of the NTA significantly suppresses the growth of the SSTAs of the El Nino events and favors an earlier peak time for the linearized El Nino events. Although the linearization of the STP and WSA tends to enhance the El Nino events' SSTAs and favors the postponement of the El Nino phase-locking time, it has relatively small effects on the SSTAs and trivially postpones phase-locking time.

The NTA, as a term superimposed on the tendency equations of the Zebiak-Cane model, induces a positive effect of nonlinearity during El Nino development (Figure 5), and therefore, enhances El Nino events. Physically, the NTA is dominantly related to the anomalous zonal SST gradient and the anomalous vertical temperature gradient (see Wang and Fang, 1996). Duan et al. (2008) demonstrated that both the anomalous zonal SST difference and the vertical temperature difference tend to increase with the development of El Nino, and the NTA also gradually increases. In other words, during an El Nino event, when the SSTA becomes large, the warming in the eastern Pacific increases the zonal SST difference and the anomalous westerly, which weakens the anomalous upwelling. The weak anomalous upwelling affects the increasing anomalous vertical temperature differ-

ence and strengthens El Niño, which implies that the nonlinearity in the NTA increases the SSTA and then hinders the decay of the linearized El Niño, favoring the phase-locking of El Niño events at the end of the calendar year. Conversely, the WSA tends to be positive during an El Niño event, namely, a westerly anomaly. However, the linearized WSA has a larger magnitude than the nonlinear WSA, which implies that the linearization favors a stronger El Niño event (Figure 5). In other words, the WSA suppresses El Niño. Meanwhile, we find that the differences between the Zebiak-Cane model and the linearized Zebiak-Cane model for sub-surface temperature tend to be negative in eastern Pacific, which indicates that the linearized sub-surface temperature for El Niño is larger than its nonlinear counterpart; in other words, the sub-surface temperature increases when the effect of nonlinearity is omitted. As a result, the temperature of upwelled water is warmer in the linearized case, which will increase the SSTA and favor a

much stronger El Niño event. Therefore, the nonlinearity related to the STP also suppresses El Niño. The nonlinearities in both WSA and STP clearly suppress El Niño and their linearization will increase the SSTA and postpone the phase-locking season of El Niño. However, the amplitude of both WSA and STP suppression on the SSTA for El Niño events is relatively small and therefore has trivial effects on the phase-locking time for the maturation of El Niño events.

In summary, the nonlinear El Niño events induced by the optimal precursory disturbances in the Zebiak-Cane model tend to phase-lock to the end of the calendar year. In contrast, the linearized El Niño events are more likely to attain peak SSTAs earlier. Nonlinearities play an important role in El Niño's mature locking to the end of the calendar year. In particular, the nonlinearities increase the SSTAs and hinder the decay of linearized El Niño events, resulting in their postponed phase-locking time and, subsequently, combined with the effect of the climatological annual cycle, causing

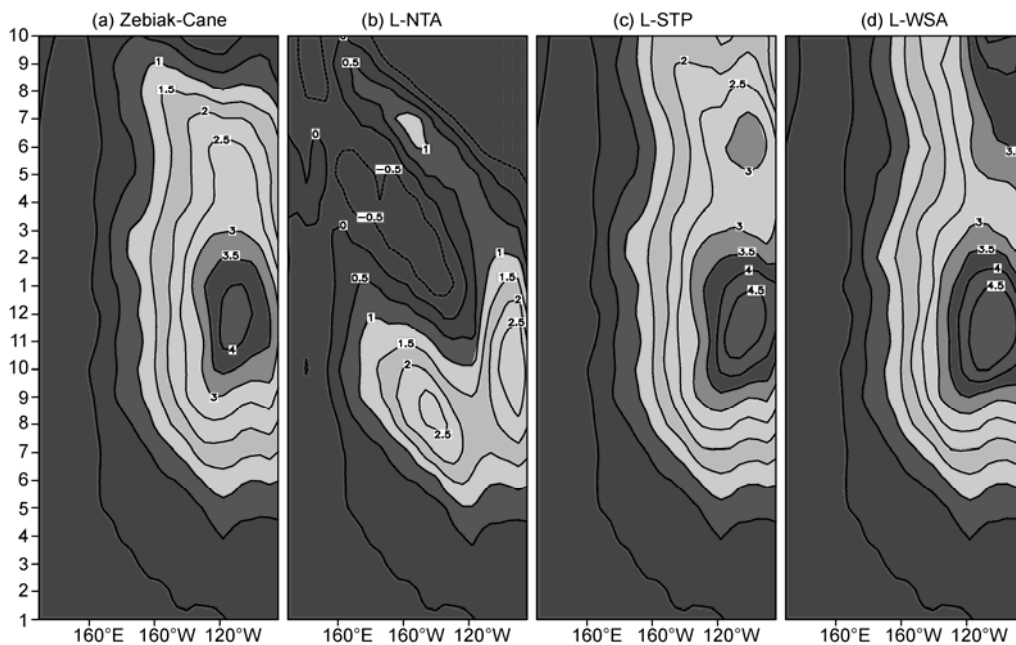


**Figure 4** SSTA components of (a) the nonlinear El Niño events with initial optimal precursory disturbance in January, (b) the El Niño events in the L-NTA model, (c) the El Niño events in the L-STP model, and (d) the El Niño events in the L-WSA model.

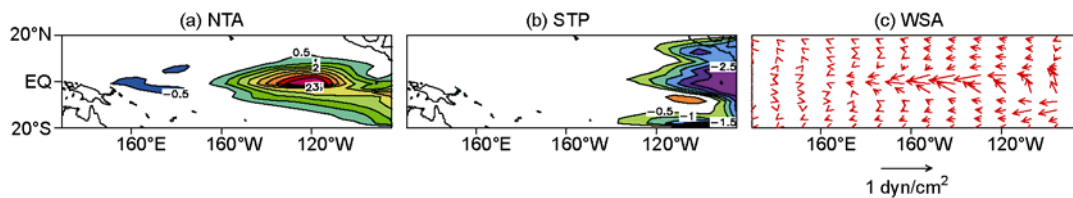


**Figure 5** Differences between the Zebiak-Cane model and the linearized Zebiak-Cane model for (a) temperature advection, (b) sub-surface temperature, and (c) wind stress. The panels show the ensemble mean of the above differences during autumn (August-September-October) when the linearized El Niño events attain peak SSTAs. This ensemble mean of the differences measures the effect of the nonlinearities (NTA, STP and WSA) on the linearized El Niño event. The positive NTA (a) values and the negative STP values (b) indicate that temperature advection and sub-surface temperature associated with the nonlinear El Niño are larger for NTA and smaller for STP than in the linearized El Niño events, which imply that linear El Niño events are enhanced by NTA and suppressed by STP. The easterly in the WSA component (c) implies that the anomalous westerly associated with nonlinear El Niño events is smaller than that associated with linearized El Niño events, suggesting that the nonlinearities in the WSA component suppress linear El Niño events.



the maturation of El Niño events at the end of the calendar year. Of the three nonlinearities in the Zebiak-Cane model that were studied here, the NTA was shown to be an essential nonlinear process that affects the phase-locking time of El Niño events.

#### 4 Summary and discussion

This paper studies the effect of nonlinearities on the phase-locking of El Niño events. We first obtain the optimal precursory disturbances of the El Niño events by computing the CNOPs of the climatological annual cycle in the Zebiak-Cane model. The conditions of the CNOPs cause them to be highly likely to evolve into El Niño events in the Zebiak-Cane model. Furthermore, these CNOP-induced El Niño events, i.e., the nonlinear El Niño events in this context, tend to lock their mature phase to the end of the calendar year. By further investigating the behaviors of El Niño events in the linearized Zebiak-Cane model, i.e., the linearized El Niño events, we find that they did not lock their mature phase to the end of a year but, rather, to the prior season. This result indicates that the nonlinearities may play a significant role in El Niño's phase-locking. In fact, we show that the nonlinearities increase SSTAs and enhance El Niño, resulting in delayed phase-locking for the El Niño events.

The nonlinearities arising from temperature advections significantly delay the phase-locking time of linearized El Niño events; in contrast, the nonlinearities in the subsurface temperature and wind stress anomalies only trivially affect El Niño's phase-locking times. Physically, the nonlinearities in temperature advections (NTA) originate from anomalous temperature advections, which are related predominantly to the anomalous zonal SST gradient and the anomalous vertical temperature gradient. Furthermore, both anomalous zonal SST differences and vertical temperature differences tend to increase (toward positive values) with the development of El Niño, and the NTA also gradually increases. In other words, during an El Niño event, when the SSTA becomes large, the warming in the eastern Pacific increases the zonal SST difference and the anomalous westerly, which weakens anomalous upwelling. The weak anomalous upwelling influences the increasing anomalous vertical temperature difference and favors the increase of the SSTA and the strengthening of El Niño, which will hinder the decay of El Niño events and postpone their phase-locking times, causing the El Niño events to lock to their mature phase at the end of the calendar year. Nonlinearities play an important role in El Niño's phase-locking and the NTA is an essential nonlinear process that modulates the ENSO's phase-locking behaviors.

As discussed in the introduction, many studies have emphasized the effect of the seasonally varying basic state on El Niño's phase-locking behaviors. Furthermore, in this

paper, we show that the nonlinearities, especially the NTA process, also play an important role in El Niño's phase-locking. It is therefore summarized that the NTA process together with the effect of the climatological annual cycle results in peak SSTA values at the end of the calendar year for El Niño events.

Although the oscillatory tendency of ENSO is now fairly well understood (see the introduction), certain aspects of the ENSO remain unclear. One aspect is the mechanism of the ENSO's irregularity. The current study identifies the effect of nonlinearity on the ENSO's phase-locking and categorizes the ENSO as a nonlinear dynamical regime. Of course, the model adopted here may be relatively simple and may not consider the complete physics of a coupled ENSO. The results may therefore be limited in regards to the model's ability to simulate a real system. In particular, because the main characteristics of La Niña events, e.g., phase-locking, cannot be well modeled by the Zebiak-Cane model (An and Wang, 2001), no attempt has been made in this paper to study the corresponding problem for La Niña events. Hence, the understanding gained from the present study needs further verification using models with more complete physics. It is expected that future studies will clearly address the ENSO's physics, including phase-locking, with more comprehensive models.

*This work was jointly sponsored by the Knowledge Innovation Program of the Chinese Academy of Sciences (Grant No. KZCX2-YW-QN203), the National Basic Research Program of China (Grant Nos. 2010CB950400 & 2012CB955202), and the National Natural Science Foundation of China (Grant No. 41176013).*

- An S-IL, Wang B. 2001. Mechanism of locking of the El Niño and La Niña mature phases to boreal winter. *J Clim*, 14: 2164–2176
- Battisti D S, Hirst A C. 1989. Interannual variability in the tropical atmosphere/ocean system: Influences of the basic state, ocean geometry and nonlinearity. *J Atmos Sci*, 46: 1687–1712
- Bjerknes J. 1969. Atmospheric teleconnections from the equatorial Pacific. *Mon Weather Rev*, 97: 163–172
- Blumenthal M B. 1991. Predictability of a coupled atmosphere-ocean model. *J Clim*, 4: 766–784
- Birgin E G, Martínez J M, Raydan M. 2000. Nonmonotone spectral projected gradient methods on convex sets, society for industrial and applied mathematics. *J Optim*, 10: 1196–1211
- Chang P, Wang B, Li T, et al. 1994. Interactions between the seasonal cycle and the Southern Oscillation: Frequency entrainment and chaos in an intermediate coupled ocean-atmosphere model. *Geophys Res Lett*, 21: 2817–2820
- Chang P, Wang B, Li T, et al. 1995. Interactions between the seasonal cycle and El Niño-Southern Oscillation in an intermediate coupled ocean-atmosphere model. *J Atmos Sci*, 52: 2353–2372
- Clarke A J, Gorder S Van. 1999. The connection between the boreal spring southern oscillation persistence barrier and biennial variability. *J Clim*, 12: 610–620
- Chen D, Cane M A, Kaplan A, et al. 2004. Predictability of El Niño over the past 148 years. *Nature*, 428: 733–736
- Duan W S, Mu M, Wang B. 2004. Conditional nonlinear optimal perturbations as the optimal precursors for El Niño-Southern Oscillation events. *J Geophys Res*, 109: D23105, doi: 10.1029/2004JD004756
- Duan W S, Mu M. 2006. Investigating decadal variability of El Niño-



- Southern Oscillation asymmetry by conditional nonlinear optimal perturbation. *J Geophys Res*, 111: C07015, doi: 10.1029/2005JC003458
- Duan W S, Xu H, Mu M. 2008. Decisive role of nonlinear temperature advection in El Nino and La Nina amplitude asymmetry. *J Geophys Res*, 113: C01014, doi: 10.1029/2006JC003974
- Duan W S, Mu M. 2009. Conditional nonlinear optimal perturbation: Applications to stability, sensitivity, and predictability. *Sci China Ser D-Earth Sci*, 52: 884–906
- Jin F F, Ghil M. 1994. El Nino on the devil's staircase: Annual subharmonic steps to chaos. *Science*, 264: 70–72
- Jin F F. 1997a. An equatorial ocean recharge paradigm for ENSO. Part I: Conceptual model. *J Atmos Sci*, 54: 811–829
- Jin F F. 1997b. An equatorial ocean recharge paradigm for ENSO. Part II: A stripped-down coupled model. *J Atmos Sci*, 54: 830–847
- Kirtman B P, Shukla J, Balmaseda M, et al. 2002. Current status of ENSO forecast skill: A report to the Climate Variability and Predictability (CLIVAR) Numerical Experimentation Group (NEG), CLIVAR Working Group on Seasonal to Interannual Prediction, *Clim. Variability and Predictability*, Southampton Oceanogr. Cent., Southampton, UK.
- Latif M, Anderson D, Barnett T, et al. 1998. A review of the predictability and prediction of ENSO. *J Geophys Res*, 103: 14375–14393
- Liu D C, Nocedal J. 1989. On the limited memory BFGS method for large scale optimization. *Mathe Program*, 45: 503–528
- Mitchell T P, Wallace J M. 1996. ENSO seasonality: 1950–78 versus 1979–92. *J Clim*, 9: 3149–3161
- Mu M, Duan W S, Wang B. 2003. Conditional nonlinear optimal perturbation and its applications. *Nonlinear Process Geophys*, 10: 493–501
- Mu M, Duan W S, Wang B. 2007a. Season-dependent dynamics of nonlinear optimal error growth and El Nino-Southern Oscillation predictability in a theoretical model. *J Geophys Res*, 112: D10113, doi: 10.1029/2005JD006981
- Mu M, Xu H, Duan W S. 2007b. A kind of initial errors related to “spring predictability barrier” for El Niño events in Zebiak-Cane model. *Geophys Res Lett*, 34: L03709, doi: 10.1029/2006GL-27412
- Mu M, Zhou F F, Wang H L. 2009. A method for identifying the sensitive areas in targeted observations for tropical cyclone prediction: Conditional nonlinear optimal perturbation. *Mon Weather Rev*, 137: 1623–1639
- Neelin J D, Jin F F, Syu H H. 2000. Variations in ENSO phase locking. *J Clim*, 13: 2507–2590
- Powell M J D. 1982. VMCWD: A FORTRAN subroutine for constrained optimization. DAMTP Report 1982/NA4, University of Cambridge, England.
- Quinn W H, Neal V T, Mayolo S E, et al. 1987. El Nino occurrences over the past four and a half centuries. *J Geophys Res*, 92: 14449–14461
- Rasmusson E, Carpenter T. 1982. Variations in tropical sea surface temperature and surface wind fields associated with the Southern Oscillation/El Nino. *Mon Weather Rev*, 110: 354–384
- Tang Y, Deng Z, Zhou X, et al. 2008. Interdecadal variation of ENSO predictability in multiple models. *J Clim*, 21: 4811–4833
- Tziperman E, Stone L, Cane M A, et al. 1994. El Nino Chaos: Overlapping of resonances between the seasonal cycle and the Pacific Ocean-Atmosphere oscillator. *Science*, 264: 72–74
- Tziperman E, Cane M A, Zebiak S E. 1995. Irregularity and locking to the seasonal cycle in an ENSO-prediction model as explained by the quasi-periodic route to chaos. *J Atmos Sci*, 52: 293–306
- Tziperman E, Zebiak S E, Cane M A. 1997. Mechanisms of seasonal-ENSO interaction. *J Atmos Sci*, 54: 61–71
- Tziperman E, Cane M A, Zebiak S E, et al. 1998. Locking of El Nino's peak time to the end of the calendar year in the delayed oscillator picture of ENSO. *J Clim*, 11: 2191–2199
- Walker G T. 1924. Correlation in seasonal variations of weather IX: A further study of world weather. *Mem Indian Meteor Dept*, 25: 275–332
- Wang B, Fang Z. 1996. Chaotic oscillations of tropical climate: A dynamic system theory for ENSO. *J Atmos Sci*, 53: 2786–2802
- Wang B, Barcilon A, Fang Z. 1999. Stochastic dynamics of El Nino-Southern Oscillation. *J Atmos Sci*, 56: 5–23
- Wang C. 2001. A unified oscillator model for the El Nino-Southern oscillation. *J Clim*, 24: 98–115
- Xue Y, Cane M A, Zebiak S E, et al. 1994. On the prediction of ENSO, a study with a low-order Markov model. *Tellus*, 46A: 512–528
- Zebiak S E. 1986. Atmospheric convergence feedback in a simple model for El Nino. *Mon Weather Rev*, 114: 1263–1271
- Zebiak S E, Cane M A. 1987. A model El Nino/Southern oscillation. *Mon Weather Rev*, 115: 2262–2278